Biophysical Chemistry 180–181 (2013) 145–152

Contents lists available at ScienceDirect

Biophysical Chemistry

journal homepage: http://www.elsevier.com/locate/biophyschem

Correlation of thermostability and conformational changes of catechol 2, 3-dioxygenases from two disparate micro-organisms

Anna Sokolova [a,*], Shir-Ly Huang [b,c], Anthony Duff [a], Elliot Paul Gilbert [a], Wen-Hsien Li [d]

[a] Bragg Institute, ANSTO, Locked Bag 2001, Kirrawee DC, NSW, 2232 Australia
[b] Department of Life Sciences, National Central University, Tao-Yuan 32001, Taiwan
[c] Center for Biotechnology & Biomedical Engineering, National Central University, Tao-Yuan 32001, Taiwan
[d] Department of Physics and Center for Neutron Beam Applications, National Central University, Tao-Yuan 32001, Taiwan

HIGHLIGHTS

- Solution structure of two C23O enzymes of different origin has been studied.
- Both C23Os present an impressive similarity in overall shape and functionality.
- Thermophilic C23O solution scattering is reproduced well from its crystal structure.
- Mesophilic C23O has a slightly extended shape in solution compared to crystal.
- Both C23Os have dramatically different thermostability and low sequence identity.

GRAPHICAL ABSTRACT

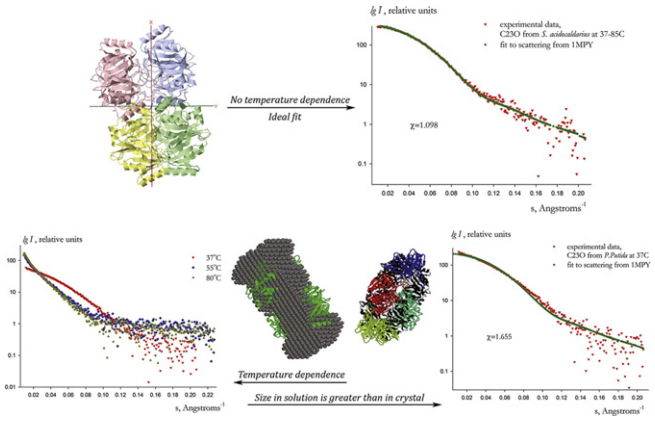

ARTICLE INFO

Article history:
Received 30 May 2013
Received in revised form 21 July 2013
Accepted 22 July 2013
Available online 3 August 2013

Keywords:
Catechol 2, 3-dioxygenase
Protein structure
Small angle X-ray scattering
Thermal effect
Modelling

ABSTRACT

We have investigated the structure of recombinant catechol 2, 3-dioxygenase (C23O) purified from two species in which the enzyme has evolved to function at different temperature. The two species are mesophilic bacterium *Pseudomonas putida* strain mt-2 and thermophilic archaea *Sulfolobus acidocaldarius* DSM639. Using the primary sequence analysis, we show that both C23Os have only 30% identity and 48% similarity but contain conserved amino acid residues forming an active site area around the iron ion. The corresponding differences in homology, but structural similarity in active area residues, appear to provide completely different responses to heating the two enzymes. We confirm this by small angle X-ray scattering and demonstrate that the overall structure of C23O from *P. putida* is slightly different from its crystalline form whereas the solution scattering of C23O from *S. acidocaldarius* at temperatures between 4 and 85 °C ideally fits the calculated scattering from the single crystal structure. The thermostability of C23O from *S. acidocaldarius* correlates well with conformation in solution during thermal treatment. The similarity of the two enzymes in primary and tertiary structure may be taken as a confirmation that two enzymes have evolved from a common ancestor.

* Corresponding author. Tel.: +61 2 9717 3606; fax: +61 2 9717 7288.
E-mail addresses: anna.sokolova@ansto.gov.au (A. Sokolova), slhuang@cc.ncu.edu.tw (S.-L. Huang), anthony.duff@ansto.gov.au (A. Duff), elliot.gilbert@ansto.gov.au (E.P. Gilbert), whli@phy.ncu.edu.tw (W.-H. Li).
URL: http://www2.ansto.gov.au/research/bragg_institute/contacts/dr_anna_sokolova (A. Sokolova).

0301-4622/$ – see front matter.
http://dx.doi.org/10.1016/j.bpc.2013.07.012

1. Introduction

Extradiol type-dioxygenases (e.g. catechol 2,3 dioxygenase or C23O) are found in a variety of bacteria and are involved in the aromatic ring fission at the *meta* position of dihydroxylated aromatics [1]. These systems are of interest from an evolutionary, geochemical and ecological perspective due to their potential application in environmental protection [2–5]. Many microorganisms are able to utilise xenobiotic aromatic compounds as the sole carbon and energy source for growth. Various effects have been made to improve their capabilities for environmental pollutant degradation and bioremediation [6].

We present here a study of two C23O enzymes of different origin: from (i) mesophilic bacteria *Pseudomonas putida* and (ii) thermophilic archaea *Sulfolobus acidocaldarius*. The two enzymes, from separate origin, present an impressive similarity in overall shape and functionality despite having dramatically different thermostability and distinguishable primary sequences. As comprehensively shown in [7], proteins adapt to higher temperatures by adopting mutations yielding increased structural stability.

P. putida is a gram-negative rod-shaped saprotrophic soil bacterium. *S. acidocaldarius* strain DSM639 belongs to the aerobic crenarchaeon and was the first hyper-thermoacidophile to be characterised from terrestrial solfataras by Brock et al. [8]. It grows optimally at 75 °C to 80 °C, at pH 2 to 3, utilising complex organic substrates. Various species can be found throughout the world in areas of volcanic or geothermal activity, such as geological formations called mud pots (or solfatare).

There are studies dedicated to determination of amino acids responsible for the thermostability of the C23O enzymes, e.g. [9,10] but the conclusions proposed there do not extend to all members of the C23O family, cf. [11]. The phylogenetic analysis of 35 extradiol dioxygenase sequences presented in [11] has revealed the evolutionary history of the enzymes. In addition, it provided a classification system and enabled conserved residues to be defined. C23O from *P. putida* is included into the set described in [11], but the sequence of C23O from *S. acidocaldarius* has not been considered. The protein sequence identity between the mesophilic and thermophilic enzymes is 31%, which is very low for making structural predictions; therefore, we determined a sequence alignment based upon the three-dimensional structural alignment of the crystal structures of the distinct C23Os reported, which represent eight different bacterial species (Table 1).

The structure of C23O from *P. putida* (Fig. 1), is one of the two structures under our investigation available at 2.8 Å resolution (PDB:1MPY, structure of catechol 2,3-dioxygenase (metapyrocatechase) from *P. putida*, [3]).

To date, little information about the high resolution structure of C23Os from thermophilic hosts is available [10,12]. Jiang et al. [13] state that the pheB gene encoding for thermostable C23O from *Bacillus stearothermophilus* has been cloned and the corresponding protein has been crystallized. The authors refer to the structural refinement and the detailed analysis of the structure and function as being in progress but, to our knowledge, the details are yet to have been published.

2. Materials and methods

2.1. Sample preparation

P. putida mt-2 was kindly provided by Dr. David T. Gibson (University of Iowa, USA). *S. acidocaldarius* DSM639 was purchased from the Bioresource Collection and Research Center (Hsin-Chu, Taiwan). The growth media and cultural conditions of these strains were according to Evans et al. [14] and Brock et al. [8], respectively.

The amplified gene fragments were subcloned into the pET28a vector (Novagen, Co.), to include N-terminal hexahistadine tags, and expressed in *Escherichia coli* BL21 (DE3) (Novagen, Co.). The recombinant strains were grown at 37 °C in Luria-Bertani medium containing kanamycin (30 μg/ml). Isopropyl β-D-1-thiogalactopyranoside (1 mM) was added to induce the expression of C23O genes.

2.1.1. Enzyme purification

The recombinant *E. coli* strains were harvested at late-log phase and the cells disrupted by sonication on ice. Clarified lysates were obtained by centrifugation at 100,000 ×*g* for 60 min at 4 °C. For protein purification, all procedures were conducted at 4 °C. C23O enzymes were purified by HisTrap affinity column (5 ml; GE Healthcare) and then on a Sephacryl S-200 HR column (145 ml, GE Healthcare) according to the manufacturer's protocols. The enzyme assay is described in [15] and the protein concentrations were determined by the Bradford method [16]. Proteins were dissolved in 50 mM Tris pH 8.0 buffer with 10% acetone used as a protein stabilizer [17,18].

2.2. Sequence alignment

The primary sequence of C23O from *S. acidocaldarius*, Uniprot: Q4J6K0, was used to BLAST [19] the PDB [20], which produced a clear set of eight cases of alignment to most of the sequence, with identity scores of 22% to 32% (Table 1). Using PROMALS3D [21], the sequence Q4J6K was then subjected to a structure based sequence alignment against eight representative structures (one for each species), using the A-chain for each structure. After rejecting one structure (PDB:1fiu) as a relative outlier, the sequence alignment shown in Fig. 3 was obtained.

2.3. SAXS data collection and processing

Small angle X-ray scattering (SAXS) data were collected on a Bruker Nanostar II SAXS camera. Protein and buffer solutions were measured using a reusable 2 mm quartz capillary. The sample volume was approximately 40 μl. The range of momentum transfer s ($s = 4\pi\sin\theta/\lambda$, where 2θ is the scattering angle and λ is wavelength = 1.54 Å using Cu K_α) was 0.01 to 0.21 $Å^{-1}$. Each data set was collected for 1 h. Sample temperature was controlled with a nominal precision of 0.1 °C.

SAXS from both C23O proteins were measured at three concentrations (9, 3 and 1.5 mg/ml) at temperatures from 4 °C to 85 °C in steps of 5 °C. At every change of the temperature, the sample was incubated for approximately half an hour with the X-ray beam off. Sample dilutions

Table 1
The sequences and structures form the PDB used in the structure based alignment by PROMALS3D. Subsequent BLASTP hits were a match to less than 50% of the length of the protein, and delineated a clear natural boundary. The last entry, Q44048, was rejected due to producing an alignment with significant insertions and deletions unlike any of the others.

Uniprot sequence	Representative PDB	BLASTP identity	Enzyme name	Species
Q4J6K0			Catechol 2,3-dioxygenase	*Sulfolobus acidocaldarius*
P06622	1mpy	31%	Metapyrocatechase	*Pseudomonas putida*
Q45135	3eck	32%	Homoprotocatechuate 2,3-dioxygenase	*Brevibacterium fuscum*
Q7WYF5	3hpy	30%	Catechol 2,3-dioxygenase	*Pseudomonas alkylphenolia*
Q0S9X1	3lm4	27%	Catechol 2,3-dioxygenase	*Rhodococcus* sp. (strainRHA1)
Q2GAG3	3b59	22%	Glyoxalase/bleomycin resistance	*Novosphingobium aromaticivorans*
Q6REQ5	2wl9	22%	Catechol 2,3-dioxygenase	*Rhodococcus* sp. DK17
P47228	1lgt	22%	Biphenyl-2,3-diol 1,2-dioxygenase	*Burkholderia xenovorans*
Q44048	1fiu	29%	3,4-Dihydroxyphenylacetate 2,3-dioxygenase	*Arthrobacter globiformis*

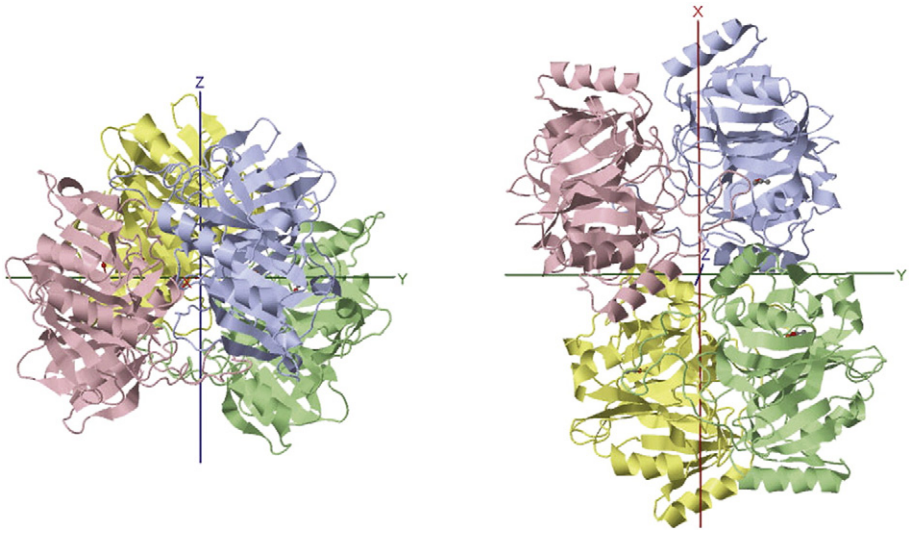

Fig. 1. Crystal structure of C23O from *Pseudomonas putida*, strain mt2. Right panel is the protein structure rotated by 90° around the horizontal axis. The quaternary structure is composed of four identical monomers.

were measured at every temperature to allow verification that the scattering curve, R_g and $I(0)/c$ were independent of concentration. Measurements were repeated prior to, and following, each 1 h run to detect possible protein damage and progressive aggregation. The scattering data were considered acceptable if there were no changes observed during 1 hour of data collection. It is important to note that, upon heating, monodisperse solutions may become polydisperse due to the protein's aggregation and denaturation. However, to demonstrate that the observed sample changes were caused only by heating and not by the variation of protein concentration or radiation damage, several solutions at different concentrations were studied. Samples were demonstrated to be stable at temperatures below 37 °C in preliminary experiments, exhibiting no changes in scattering with the time of incubation. Scattering from pure buffer was measured at the same temperatures as the proteins. Scattering data from commercially available bovine serum albumin (BSA) dissolved in HEPES at pH7.5 following the standard protocol ensuring monodispersity of the final solution, and verification of the correct R_g, these data were used as an intensity standard to define molecular weight (MW) of the C23Os. In addition, the MW for the species in solution has been estimated using the experimental value of their excluded volume V directly calculated from SAXS data. V can be determined [22] using the Porod Eq. (1) [23], where ρ is the scattering density distribution within the single particle, S is its surface area, Q is the Porod invariant and K_4 is a constant determined to ensure that the asymptotical intensity decay is proportional to s^{-4} at higher angles.

$$\lim_{s\to\infty} I(s) = \frac{2\pi}{s^4}\rho^2 S;\quad V = \frac{2\pi^2 I(0)}{Q},\quad Q = \int_0^\infty [I(s) - K_4]s^2 ds \tag{1}$$

The forward scattering $I(0)$, maximum dimension D_{max}, distance distribution functions $p(r)$ (Eq. (2)), and radii of gyration R_g were evaluated with the indirect transform package GNOM [24].

$$p(r) = \frac{1}{2\pi^2}\int_{s=0}^{D_{max}} I(s)\cdot\frac{\sin(sr)}{sr} ds \tag{2}$$

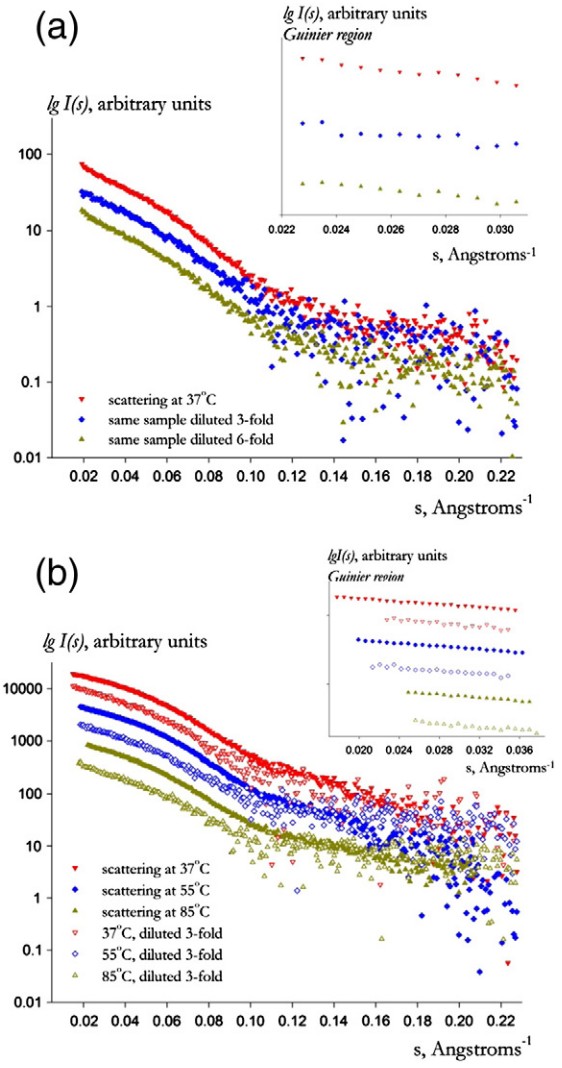

Fig. 2. Selected scattering patterns and corresponding Guinier regions shown on insets. (a) Data from C23O (*P. putida*) solution at 37 °C and from two samples dilute 3-fold and 6-fold; (b) data from C23O (*S. acidocaldarius*) collected at 37 °C, 55 °C and 85 °C and the same solution at the same temperatures diluted 3-fold.

```
     1       10        20        30        40        50        60
 1   MNKGVMRPGHVQLRVLDMSKALEHYVELLGLIEMDRDDQGRVYLKAWTEVDKFSLVLREA   60
 1   -MSEVLRLSHVCVRVIDMDKSLFFYRDLLGFHETEKNG-DYVYLRGYEEGQHHSLVLKRA   58

61   DEPGMDFMGFKVVDEDALRQLERDLMAYGCAVEQLPAGELNSCGRRVRFQAPSGHHFELY  120
59   ESPGLSYIAFRVRN---VDKMREKLEASGLKTRKFEE---KGVDNAIIFSDTGGMPTVFY  112

121  ADKEYTGKWGLNDVNPEAWPRDLKGMAAVRFDHALMYG-DELPATYDLFTKVLGFYLAEQ  179
113  ENMEYVDD-------IRMKFHIHKGVSPIRLAHVNLMVDSNVFENEIKFYQSLGFYETEI  165
                                        *
180  VLDENGTRVAQFLSLSTKAHDVAFIHHPEK-GRLHHVSFHLETWEDLLRAADLISMTDT-  237
166  FLDKEGKKMVSWLTKSGDSHNLAISKSSRKTPGFHHFTYYVHDLRDVIRAADIMASAELW  225
                      *               *
238  -SIDIGPTRHGLTHGKTIYFFDPSGNRNEVFCGGDYNYPD--HKPVTWTTDQLGKAIFYH  294
226  DYIERGPGRHGVTQGVYIYLRDPNGGRLEFFTGDYVVLDPDKWKPVVWTYEQFRYRSDYW  285
               *         *         *
295  DRILNERFMTVLT---------------  307
286  SRPIPESWLNEWIPVEDPFTGNLRGWNT  313
```

Fig. 3. Top line: catechol 2,3-dioxygenase from *Pseudomonas putida* (PDB:1MPY). Second line: catechol 2,3-dioxygenase from *Sulfolobus acidocaldarius* β-sheet indicated in blue; α-helix indicated in red. The active site Fe(II) ligands are indicated with an "*".

To verify the data quality and consistency of the obtained results, R_g were also estimated independently using the Guinier approximation (3) using the software PRIMUS [25].

$$I(s) = I(0)e^{-\frac{s^2R_g^2}{3}} \tag{3}$$

Additionally, to get further confirmation of MW values, we have used a new method recently described in [26]. In short, MW is defined by empirical equation:

$$MW = \left(\frac{I(0)}{\int_0^\infty s \cdot I(s)ds} \right)^2 \cdot 0.1231 \cdot R_g \tag{4}$$

Fig. 2 shows representative sets of scattering from both proteins in non-aggregated, non-denatured conditions. Panel (a) is a concentration series, from C23O from *P. putida* at the 37 °C with the Guinier regions shown in the inset. Points at very low *q* have been truncated, removing sharp upright in the data. Based on DLS data, we believe that the amount of aggregation was very small, involving very large aggregate particles, and their effect on the data was confined to very low Q (up to 0.02 $Å^{-1}$). Panel (b) shows three dilution pairs for *S. acidocaldarius* at three temperatures, and the inset presents Guinier regions for the data. *Rg* and *I*(0) within the concentration series are consistent, confirming stability of the samples. To confirm the monodispersity of the samples (in other words, to confirm that patterns are equivalent), Singular Value Decomposition methodology (SVD) [25] has been implemented. For both enzymes, SVD gave only one component presented in the series of scattering data.The scattering intensity from prokaryotic C23O was computed using CRYSOL [27].

It is known [28,29] that the presence of His-tags can potentially change the scattering profile of the protein to which they are attached. The effect, however, is dependent on the relative size of the His-tag. The addition of a six amino acid His-tag would have little effect on the proteins in the current study given their >300 amino acid structure; nonetheless, for completeness, we modelled the influence of attaching His-tag to the C23O from *P. putida* molecule and determined the associated scattering structure using MASSHA [30] and CRYSOL [27]. It is evident that the His-tag addition has no significant effect on the overall scattering.

2.4. Shape reconstruction by simulated annealing

The shape of C23O from *P. putida* was restored from the scattering from a monodisperse solution of the protein using an *ab initio* shape determination method implemented in the program DAMMIF [22]. The method searches for a compact interconnected configuration of dummy atoms, the scattering which minimizes the discrepancy χ^2 between the calculated and the experimental curves:

$$\chi^2 = \frac{1}{N-1}\sum_j \left[\frac{I(s_j) - I_{exp}(s_j)}{\sigma(s_j)} \right]^2 \tag{5}$$

where *N* is the number of experimental points, and $I_{exp}(s_j)$ and $\sigma(s_j)$ are the experimental intensity and its standard deviation measured at the momentum transfer s_j, respectively, and $I(s_j)$ is the scattering intensity from the model.

2.5. Shape reconstruction by rigid body modelling

A rigid body modelling technique was used to build the tentative model of C23O from *P. putida*. The program, SASREF [31], which performs quaternary structure modelling of a complex formed by subunits with known structure against the SAXS data set, was implemented. The program uses partial scattering amplitudes of the subunits precomputed by the program CRYSOL [27].

3. Results and discussion

3.1. Primary sequence alignment

To check if the findings in [10] are applicable to the C23O from *S. acidocaldarius*, the sequence alignment for the two proteins in the current study has been determined. Despite a low sequence identity of 31%, an excellent alignment of secondary structure elements is evident (Table 1 and Fig. 3). The active site residues are completely conserved amongst the selected structures.

3.2. Structure of C23O from P. putida strain mt2

Three typical scattering patterns measured at 37 °C, 55 °C and 85 °C are shown in Fig. 4(a). The profile of scattering at 37 °C illustrates the behaviour dictated by Porod's law (1), i.e. dependence of $I(s)$ from s^{-4} is virtually flat. Such behaviour indicates that particles in solution have a smooth and sharp interface with solvent. Upon heating, the overall parameters of the particle increase up to $R_g = 125 \pm 5$ Å and $D_{max} = 400 \pm 20$ Å for 85 °C (Table 2). The signature of denaturation should

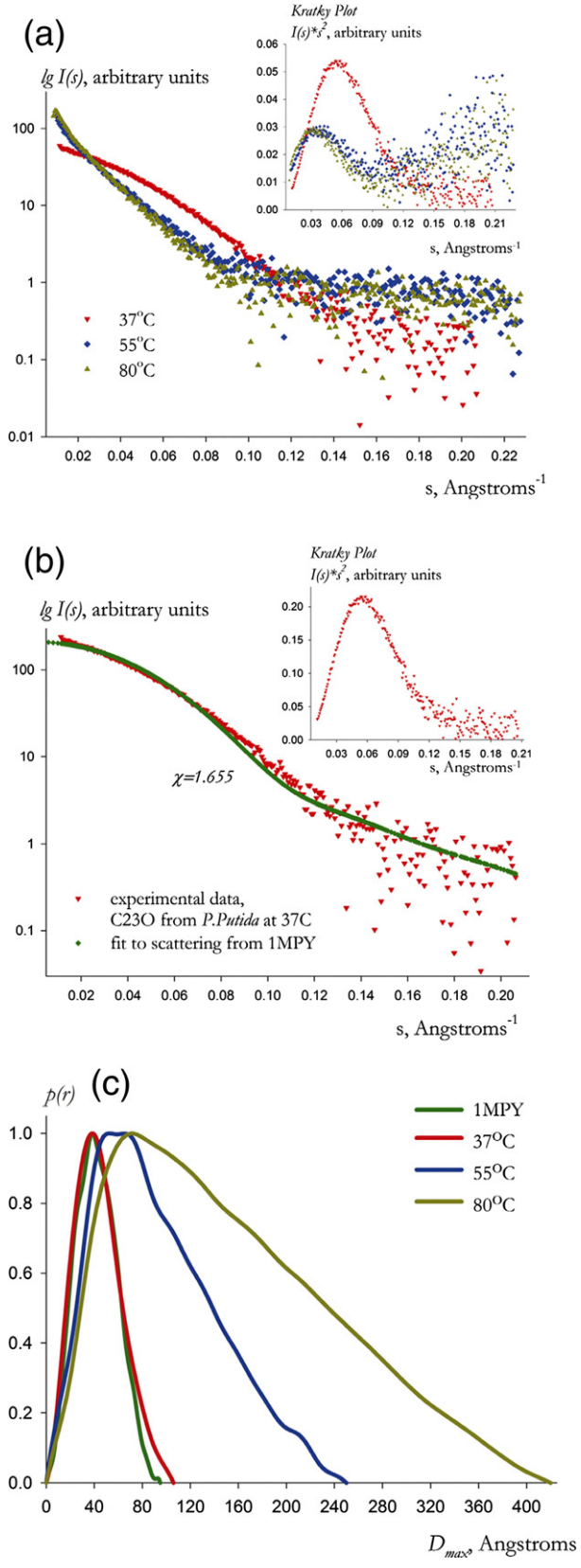

Fig. 4. (a) Measured scattering profiles for C23O, *Pseudomonas putida*, strain mt2, at 37 °C, 55 °C and 85 °C and corresponding Kratky plots; (b) experimental SAXS profile for prokaryotic C23O fitted by intensity calculated by CRYSOL from its crystal structure 1MPY and Kratky plot; (c) *p(r)* functions for prokaryotic C23O in crystal (green pattern) and in solution and for the protein heated up to 37 °C, 55 °C and 85 °C.

Table 2
Structural and fitting parameters for C23O (*P. putida*) and C23O (*S. Acidocaldarius*).

	C23O *P. putida*			C23O *S. acidocaldarius*	1MPY
	37 °C	55 °C	85 °C		
DLS: fractions at $R_h = 30 \pm 5$ Å	96 ± 2% (by intensity)			96 ± 2% (by intensity)	–
R_g (Å)	35 ± 2	75 ± 5	125 ± 5	33 ± 1	32 ± 1
D_{max} (Å)	110 ± 5	250 ± 10	400 ± 20	97 ± 3	94 ± 2
MW (kDa), calculated by $I(0)$ analysis	150 ± 20			150 ± 20	–
MW (kDa), calculated from excluded volume analysis	130 ± 10			135 ± 10	–
χ, CRYSOL fit	1.6			1.1	–
χ, rigid body fit	1.1			–	–

be reflected in the scattering in the limit of low angles. For denatured proteins, Kratky's law plot (6):

$$\lim_{s\to\infty} s^2 \cdot I = \frac{2}{R_g^2}\left(1-\frac{1}{s^2 R_g^2}\right) \quad (6)$$

i.e. $I(s)\cdot s^2$, should be effectively smooth without pronounced peaks. Data collected from heated solutions show some evidence of protein denaturation but at the same time still presents a clear peak at higher *s* on a Kratky plot (Fig. 4). $p(r)$ functions also show the presence of compact globular particles in solution.

These data show that C23O from *P. putida* mt2 is stable at temperatures up to ~40 °C. At these conditions, R_g and D_{max}, calculated from experimental data, are larger than the values calculated from the crystal structure (Table 2). At higher temperatures, the shape of the SAXS patterns dramatically differs.

Monodispersity of the *P. putida* in solution cannot be maintained upon heating, so *ab initio* models could not be generated for this mesophilic protein at temperatures higher than 37 °C. To analyse the tendency of an increase of the particle's size in solution upon heating, Fourier analysis (2) was implemented. Effective values of R_g and D_{max} have been calculated to quantitatively characterise the changes. Fig. 4(c) shows a continuous change of $p(r)$ with heating for scattering data shown in Fig. 4(a). Observed behaviour indicates that the protein either aggregated, or aggregated and partially denatured. Non-reversible clouding of the sample was observed at temperatures above 80 °C.

Recently [15], small angle neutron scattering has been employed to investigate the temperature-dependent solution structure of C23O from *P. putida*, strain SH1 up to 80 °C. There is 94% identity of C23O from strain SH1 compared to that from strain mt2. The authors show that the native enzyme from strain SH1 in solution has the same size as the crystal structure of C23O from *P. putida*. The authors also report non-reversible enlargement of the protein shape at temperatures higher than 50 °C, and proposed that at these higher temperatures, the protein dissociates into dimers and further denatures.

In contrast, we show here using SAXS that there is no evidence for such dissociation. Statistical noise at high angles limits more detailed assessment of conformational changes. Kratky plots for scattering data measured at 37 °C, 55 °C and 85 °C shown in Fig. 4(a) indicate that the protein becomes slightly less compact at higher temperatures, but still is compact and retain their shape.

To define the shape of the enzyme in solution at temperatures below or equal to 37 °C, attempts were made to fit the SAXS from C23O from *P. putida* mt2 by the profile calculated for crystal structure PDB:1MPY; however this fit was poor (Fig. 4(b)). To confirm the mismatch of experimental and calculated structures, $p(r)$ functions extracted from both patterns are shown in Fig. 4(c). The application of

ab initio reconstruction to scattering from monodisperse solutions at T ≤ 37 °C gave a structure shown in Fig. 5 (left panel). Relaxation of the symmetry during the use of rigid body modelling yielded the structure shown in Fig. 5 (right panel). These reconstructions are presented as illustrations of conformation and confirmation of the fact that mesophilic structure is much less compact compared to its thermophilic analogue. R_g of the protein in solution increases with heating from 35 Å to 125 Å. Restoration (use of *ab initio* and rigid body approaches) of the protein's shape at higher temperatures is impossible because of lack of information about the oligomeric composition of the solutions of C23O from *P. putida* mt2.

3.3. Structure of C23O from S. acidocaldarius strain DSM639

The structure of thermophilic C23O remains unchanged up to temperatures of 85 °C. The crystal structure of this protein is unavailable therefore the crystal structure PDB:1mpy was used as a basis for modelling the enzyme despite significant differences in primary sequence. As shown in Fig. 6, SAXS from thermophilic C23O is extremely well fitted by the calculated profile from crystal structure 1MPY with the thermophilic protein having a shape in solution identical to bacterial C23O in the crystal. Indeed, the DaRa algorithm identifies molecule 1MPY.pdb to be its closest structural homologue [32]. The overall parameters of the two proteins match very well (Table 2).

The observed constancy of the C23O (*S. acidocaldarius*) structure over a wide range of temperatures and its overall structural identity to the crystallised homologue C23O (*P. putida*) (cf. Table 1) leads us to postulate that thermostability is associated with more compact structures that are more typical of a crystal structure.

We propose that the clearly pronounced difference between the subunit arrangement in solution and in the crystal is caused by intermolecular mobility. Such discrepancy has been reported in numerous studies [33] and can be attributed to the influence of the crystal packing forces on the arrangement of monomers within complex structures.

4. Conclusions

We have investigated the structure of two C23O enzymes, one from mesophilic bacteria and another from thermophilic archaea as a function of temperature.

At a fundamental level, this study demonstrates the role of enhanced stability as a function of temperature with respect to the corresponding host-preferred temperature. It is well accepted in the literature [for example, 34] that thermophiles have enhanced stability in terms of structural globularity. It is shown that temperature increase above the host-preferred temperature leads to unfolding of the protein. It is confirmed by molecular dynamics methods that thermophilic proteins are more rigid in comparison to their mesophilic homologues. It has been found that the local networks of salt bridges and hydrogen bonds in thermophiles render their structure more stable with respect to fluctuations of individual contacts.

We find that the solution shape of C23O from the mesophilic bacterium is larger than that of its corresponding crystal form. In contrast, the shape of thermophilic C23O is reproduced well by the shape of crystalline C23O from *P. putida*. The explanatory interpretation is that the mesophile protein is enlarged in solution due to greater flexibility at ambient to warm temperatures, while the thermophile protein remains compact, as if cold, at sub-thermophilic temperatures [35].

We also find that the observed stability of the C23O from *S. acidocaldarius* can be explained by the presence of a set of residues surrounding the active center of the enzymes. A structure-based sequence alignment of extradiol-type dioxygenases reveals that catalytically and structurally important amino acid residues of the enzymes were conserved during evolution. A sequence comparison of catechol 2, 3-dioxygenase with other extradiol-type dioxygenases leads to the identification of evolutionally conserved amino acid residues whose possible catalytic roles have been proposed [36]. In light of the evolutionary relationship between mesophilic and thermophilic C23O enzymes whose catalytic mechanisms are conserved; unravelling such structural differences between these two representatives of bacterial and archaea hosts will provide a better understanding of enzyme evolution.

Acknowledgements

The authors thank Dr Robert Knott (Bragg Institute, ANSTO) and Dr Tracey Hanley (Institute of Materials Engineering, ANSTO) for the extremely useful and fruitful discussions of the SAXS data. We appreciate the help of Dr Agata Rekas (National Deuteration Facility, ANSTO) for the control of the samples' quality prior the SAXS experiments.

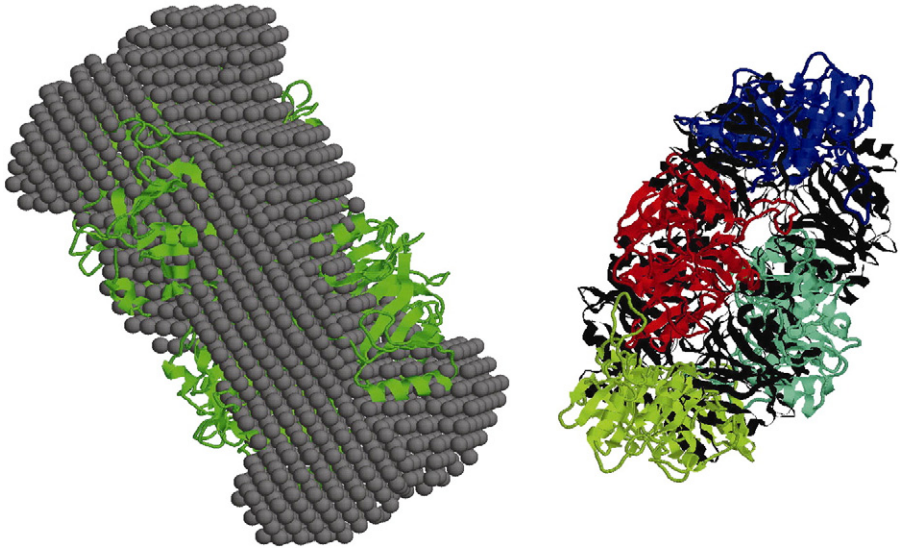

Fig. 5. Left panel: dummy atom model (grey) and 1MPY structure (green); right panel: rigid body model, no symmetry maintained in modelling and 1MPY (black).

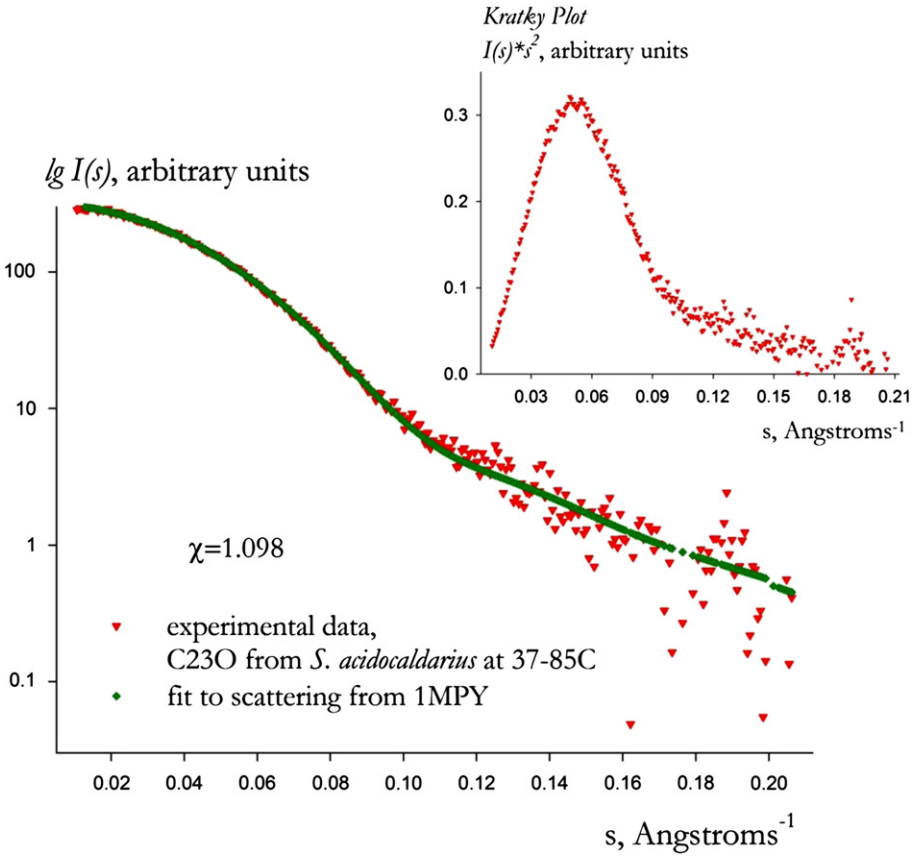

Fig. 6. Experimental SAXS profile for thermophilic C23O fitted by intensity calculated by CRYSOL from the crystal structure PDB:1MPY and corresponding Kratky plot.

The authors thank the grant support from National Science Council in Taiwan (NSC-97-2317-B-008-003) for the preparation of enzyme samples.

References

[1] T. Ishida, A. Kita, K. Miki, M. Nozaki, K. Horiike, Structure and reaction mechanism of catechol 2,3-dioxygenase (metapyrocatechase), International Congress Series 1233 (2002) 213–220.
[2] S. Han, L.D. Eltis, K.N. Timmis, S.W. Muchmore, J.T. Bolin, Crystal structure of the biphenyl-cleaving extradiol dioxygenase from a PCB-degrading pseudomonad, Science 270 (1995) 976–980.
[3] A. Kita, S. Kita, I. Fujisawa, K. Inaka, T. Ishida, K. Horiike, M. Nozaki, K. Miki, An archetypical extradiol-cleaving catecholic dioxygenase: the crystal structure of catechol 2,3-dioxygenase (metapyrocatechase) from *Pseudomonas Putida* mt-2, Structure 7 (1999) 25.
[4] F.M. Duffner, U. Kirchner, M.P. Bauer, R. Müller, Phenol/cresol degradation by the thermophilic *Bacillus thermoglucosidasius* A7: cloning and sequence analysis of five genes involved in the pathway, Gene 256 (2000) 215.
[5] D.J. Hassett, U.A. Ochsner, S.L. Groce, K. Parvatiyar, J.F. Ma, J.D. Lipscomb, Hydrogen peroxide sensitivity of catechol-2,3-dioxygenase: a cautionary note on use of xylE reporter fusions under aerobic conditions, Applied and Environmental Microbiology 66 (2000) 4119.
[6] M. Dua, A. Singh, N. Sethunathan, A.K. Johri, Biotechnology and bioremediation: successes and limitations, Applied Microbiology and Biotechnology 59 (2002) 143.
[7] A. Szilágyi, P. Závodszky, Structural differences between mesophilic, moderately thermophilic and extremely thermophilic protein subunits: results of a comprehensive survey, Structure 8 (2000) 493.
[8] T.D. Brock, K.M. Brock, R.T. Belly, R.L. Weiss, Sulfolobus: a new genus of sulphur-oxidizing bacteria living at low pH and high temperature, Archiv für Mikrobiologie 84 (1972) 54.
[9] Z. Guo, L.N. Xu, L.X. Zhou, The mechanism of TC23O's thermostability: a molecular dynamics simulation study, Journal of Biomolecular Structure and Dynamics 23 (2006) 603.
[10] L. Dai, C. Ji, D. Gao, J. Wang, T. Jiang, A. Bi, X. Sheng, Y. Mao, Modeling and analysis of the structure of the thermostable catechol 2,3-dioxygenase from *Bacillus stearothermophilis*, Journal of Biomolecular Structure and Dynamics 19 (2001) 75.
[11] L.D. Eltis, J.T. Bolin, Evolutionary relationships among extradiol dioxygenases, Journal of Bacteriology 178 (1996) 5930.
[12] M.Q. Chen, C.C. Yin, W. Zhang, Y.M. Mao, Z.H. Zhang, Purification, crystallization and preliminary X-ray diffraction studies of the thermostable catechol 2,3-dioxygenase of *Bacillus stearothermophilus* expressed in *Escherichia coli*, Acta Crystallographica D54 (1998) 446.
[13] T. Jiang, C. Ji, X. Sheng, M. Chen, Y. Xie, W. Gong, Y. Ma, Crystal structure of thermostable catechol 2,3-dioxygenase determined by multiwavelength anomalous dispersion method, Chinese Science Bulletin 47 (2002) 307.
[14] P.J. Evans, D.T. Mang, L.Y. Young, Degradation of toluene and *m*-xylene and transformation of *o*-xylene by denitrifying enrichment cultures, Applied and Environmental Microbiology 57 (1991) 450.
[15] S.L. Huang, Y.C. Hsu, J.W. Lynn, S.Y. Wu, W.H. Li, Thermal effects on the activity and structural conformation of catechol 2,3-dioxygenase from *Pseudomonas putida* SH1, The Journal of Physical Chemistry B 114 (2010) 987.
[16] M.M. Bradford, A rapid and sensitive method for the quantitation of microgram quantities of protein utilizing the principle of protein-dye binding, Analytical Biochemistry 72 (1976) 248.
[17] C. Nakai, K. Hori, H. Kazuko, H. Kagamiyama, T. Nakazawa, M. Nozaki, Purification, subunit structure, and partial amino acid sequence of metapyrocatechase, Journal of Biological Chemistry 258 (1983) 2916.
[18] C. Nakai, H. Kagamiyama, M. Nozaki, T. Nakazawa, S. Inouye, Y. Ebina, A. Nakazawa, Complete nucleotide sequence of the metapyrocatechase gene on the TOL plasmid of *Pseudomonas putida* mt-2, Journal of Biological Chemistry 258 (1983) 2923.
[19] S.F. Altschul, W. Gish, W. Miller, E.W. Myers, D.J. Lipman, Basic local alignment search tool, Journal of Molecular Biology 215 (1990) 403, (http://blast.ncbi.nlm.nih.gov).
[20] F.C. Bernstein, T.F. Koetzle, G.J.B. Williams, E.F. Meyer Jr., M.D. Brice, J.R. Rodgers, O. Kennard, T. Shimanouchi, M. Tasumi, The Protein Data Bank: a computer-based archival file for macromolecular structures, Journal of Molecular Biology 112 (1977) 535.
[21] J. Pei, B.-H. Kim, N.V. Grishin, PROMALS3D: a tool for multiple sequence and structure alignment, Nucleic Acids Research 36 (2008) 2295–2300.
[22] D. Franke, D.I. Svergun, DAMMIF, a program for rapid shape determination in small-angle scattering, Journal of Applied Crystallography 42 (2009) 342.
[23] G. Porod, General Theory. Small-angle X-ray Scattering, in: O. Glatter, O. Kratky (Eds.), Academic Press, London, 1982, pp. 17–51.
[24] D.I. Svergun, Determination of the regularization parameter in indirect-transform methods using perceptual criteria, Journal of Applied Crystallography 25 (1992) 495.
[25] P.V. Konarev, V.V. Volkov, A.V. Sokolova, K.M.J. Koch, D.I. Svergun, PRIMUS — a Windows-PC based system for small-angle scattering data analysis, Journal of Applied Crystallography 36 (2003) 1277.

[26] R. Rambo, J. Tainer, Accurate assessment of mass, models and resolution by small-angle scattering, Nature 496 (2013) 477.
[27] D.I. Svergun, C. Barberato, M.H.J. Koch, CRYSOL — a program to evaluate X-ray solution scattering of biological macromolecules from atomic coordinates, Journal of Applied Crystallography 28 (1995) 768.
[28] G.L. Hura, A.L. Menon, M. Hammel, R.P. Rambo, F.L. Poole, S.E. Tsutakawa, F.E. Jenney Jr., S. Classen, K.A. Frankel, R.C. Hopkins, S. Yang, J.W. Scott, B.D. Dillard, M.W.W. Adams, J.A. Tainer, Robust, high-throughput solution structural analyses by small angle X-ray scattering (SAXS), Nature Methods 6 (2009) 606.
[29] M. Pelikan, G.L. Hura, M. Hammel, Structure and flexibility within proteins as identified through small angle X-ray scattering, General Physiology and Biophysics 28 (2009) 174–189.
[30] P.V. Konarev, M.V. Petoukhov, D.I. Svergun, MASSHA — a graphic system for rigid body modelling of macromolecular complexes against solution scattering data, Journal of Applied Crystallography 34 (2001) 527–532.
[31] M.V. Petoukhov, D.I. Svergun, Global rigid body modelling of macromolecular complexes against small-angle scattering data, Biophysical Journal 89 (2005) 1237.
[32] A.V. Sokolova, V.V. Volkov, D.I. Svergun, Prototype of a database for rapid protein classification based on solution scattering data, Journal of Applied Crystallography 36 (2003) 865, (dara.embl-hamburg.de).
[33] D.I. Svergun, Small-angle X-ray and neutron scattering as a tool for structural systems biology, Biological Chemistry 391 (2010) 737.
[34] T.B. Mamonova, A.V. Glyakina, O.V. Galzitskayab, M.G. Kurnikova, Stability and rigidity/flexibility — two sides of the same coin? Biochimica et Biophysica Acta (BBA) — Proteins and Proteomics 854 (2013) 854.
[35] C.S. Kealley, A.V. Sokolova, G.J. Kearley, E. Kemner, M. Russina, A. Faraone, W.A. Hamilton, E.P. Gilbert, Dynamical transition in a large globular protein: macroscopic properties and glass transition, Biochimica et Biophysica Acta 1 (2010) 34.
[36] J. Lee, L. Oh, K.R. Min, C.K. Kim, K.H. Min, K.S. Lee, Y.C. Kim, J.Y. Lim, Y. Kim, Structure of catechol 2,3-dioxygenase gene encoded in chromosomal DNA of *Pseudomonas putida*, Biochemical and Biophysical Research Communications 224 (1996) 831.